Theor Appl Climatol (2009) 96:221–233
DOI 10.1007/s00704-008-0026-4

ORIGINAL PAPER

Investigation of aerosol optical properties in Bangkok and suburbs

S. Janjai · S. Suntaropas · M. Nunez

Received: 5 June 2007 / Accepted: 12 March 2008 / Published online: 17 April 2008
© Springer-Verlag 2008

Abstract Aerosol optical depth and Angstrom coefficients for three sites in Bangkok and suburbs are examined: Silpakorn University at Nakhon Pathom, NP (13.82°N, 100.04°E), the Asian Institute of Technology at Phatum Thani, AIT (14.08°N, 100.62°E) and the Thai Meteorological Department at Bangkok, BK (13.73°N, 100.57°E). Sunphotometers have been used to measure direct normal spectral irradiance at these sites for a period of 2 years (2004–2005). Cloudless conditions were selected and Bouguer's law was employed to obtain aerosol optical depth. All three sites exhibit strong seasonal variations, with the highest values occurring at the height of the dry season in April, and the lowest occurring during the rainy season in July. April turbidity conditions are very high, as evidenced by maximum 500 nm optical depths of between 1.4 to 2.0 that were measured at all three locations. The Angstrom exponent α also showed a marked seasonal change, with highest values at the height of the dry season.

Nomenclature

$I_{o\lambda}$	Extraterrestrial solar irradiance
I_a	Modelled direct irradiance at the surface with aerosols
I_0	Modelled direct irradiance at the surface without aerosols
D_a	Modelled diffuse irradianxce at the surface with aerosols
D_0	Modelled diffuse irradiance at the surface without aerosols
G_a	Modelled global irradiance at the surface with aerosols
G_0	Modelled global irradiance at the surface without aerosols
G_m	Measured global irradiance at the surface
R	Correlation coefficient
SD	Standard deviation
m_r	Relative air mass
τ'_λ	Total atmospheric optical depth
$\tau'_{a\lambda}$	Optical depth due to aerosol scattering and absorption
$\tau'_{g\lambda}$	Optical depth due to the atmospheric gases absorption
$\tau'_{o\lambda}$	Optical depth due to the ozone absorption
$\tau'_{r\lambda}$	Optical depth due to Rayleigh scattering
$\tau'_{w\lambda}$	Optical depth due to the water vapour absorption
α'	Wavelength exponent
β	Angstrom's turbidity coefficient
λ	Wavelength

S. Janjai (✉) · S. Suntaropas
Laboratory of Tropical Atmospheric Physics,
Department of Physics, Faculty of Science,
Silpakorn University,
Nakhon Pathom 73000, Thailand
e-mail: serm@su.ac.th

M. Nunez
School of Geography and Environmental Studies,
University of Tasmania,
Sandy Bay 7005 Tasmania, Australia

1 Introduction

Bangkok, the capital of Thailand, is typical of many urbanized locations in the recently developed world experiencing unprecedented growth. The present population of the Bangkok metropolitan area, which encompasses five surrounding provinces has doubled in the last two decades with a present population of just under 10 million. It has an area of 7,761 km^2 which has rapidly industrialized, and

which houses a range of government, industrial and commercial infrastructures. This development has attracted a large population and the wide use of privately owned automobiles. These pressures from urbanization affect the character and quality of the environment, which in turn may affect the climate of the region such as its precipitation, solar radiation or potential evaporation (Oke 1987). In this study, we examine what effect aerosols are having in depleting solar radiation over Bangkok. This is accomplished by sunphotometer measurements at three locations in the Bangkok area.

Aerosols are small particles suspended in the atmosphere for indefinite periods of time. They may have profound effects on human health by virtue of their ability to be inhaled in the lungs if the particles are sufficiently small (Oke 1987; NEPC 1997). Their effect on the physical environment can also be important as they have the ability to scatter or absorb incident solar radiation. At the regional scale they may relate to material degradation, affect atmospheric stability and air motion, reduce solar radiation reaching the earth's surface and the rate of potential photosynthesis. At the global scale they are believed to be efficient scattering agents, cooling the globe and partly counteracting the effect of greenhouse warming as well as significantly influencing the hydrological cycle (Xin et al. 2005).

Optical measurements of atmospheric aerosols usually involve measurements of direct solar radiation in distinct spectral bands using pyrheliometers or sunphotometers (Iqbal 1983). These measurements may be used to obtain aerosol optical depth (AOD) and the Angstrom turbidity coefficient as will be described in the next section (Masmoudi et al. 2003; Angstrom 1929, 1964; Ramachandran and Jayaraman 2003). These measurements are complicated as aerosols are noted for their variability in space and time, making it difficult to produce aerosol climatologies. Kaufman et al. (1994) argues the need to measure aerosol characteristics at different locations and in various meteorological conditions to fully assess regional aerosol properties. For many tropical regions, aerosols from biomass burning and urbanization have become more important to the climate of these regions (Von Hoyningen-Huene et al. 1999). Accurate information on aerosols is required for understanding the effects of aerosols on the climate system and its variation in these regions.

Despite the obvious need for aerosol data, there are very few measurements of this type taken in tropical cities. In Bangkok, there are no systematic long-term studies of aerosol optical properties that have been published to date. In this study, we present a 2-year data set from three sunphotometers located at different locations in Bangkok. Seasonal features, if any, are expected to manifest themselves as will any regional variability. While the study does not meet the long-term criteria of a climatology, it does nevertheless provide useful data on aerosol characteristics, their amount, and variability at this point in time.

2 Instrumentation and measurement details

Measurements were carried out in Silpakorn University, at Nakhon Pathom (NP), a town located some 60 km west of Bangkok, but now taken over by the city's suburban sprawl (Fig. 1). A Yankee MFRSR (model MO249), installed on the roof of the Science Building, measured global, diffuse, and direct narrow-band spectral irradiance in six wavelength intervals (Table 1). Only the five lowest wavelength bands are used in the analysis as the 940-nm channel is influenced by water vapour absorption. Continuous measurements were taken from the period January 2004 to December 2005 with a sampling interval of 24 s. The second set of measurements was taken at the Asian Institute

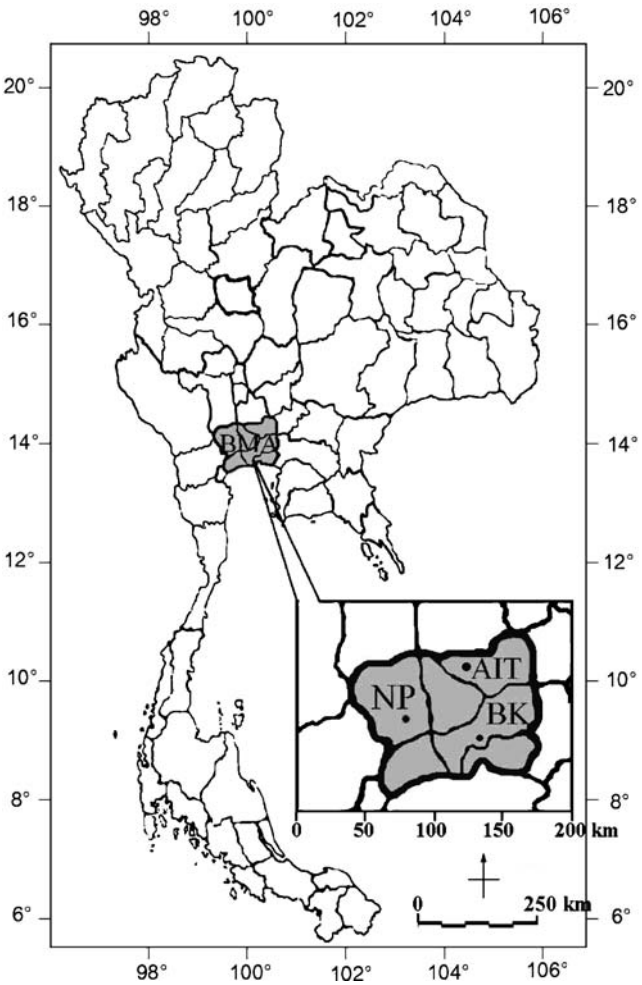

Fig. 1 Map of Thailand showing the three measurement sites at Silpakorn University in Nakhon Pathom (*NP*), Asian Institute of Technology in Phatum Thani (*AIT*) and Bangkok (*BK*). Area in *heavy line* encompasses Bangkok and the five provinces which make up the Bangkok metropolitan area

Table 1 Measurement details

Location	Latitude	Longitude	Instrument	B_1	B_2	B_3	B_4	B_5	B_6
Nakhon Pathom (NP)	13.82°N	100.04°E	Yankee MFRSR	413	500	613	671	863	940
Phatum Thani (AIT)	14.08°N	100.62°E	EKO MS-110	368	500	675	778	863	–
Bangkok (BK)	13.73°N	100.57°E	CIMEL CE 317	380	440	500	670	870	937

All wavelength bands (B_i) are given in nanometers

of Technology (AIT) Campus in Phatum Thani province, just 40 km north of Bangkok. An EKO sunphotometer (model MS-110) was used to measure spectral irradiance on the roof of a two-storey building housing offices of the Energy Program. Measurements were taken in five wavelength bands (Table 1), at a frequency of 1 min and over a 2-year period as in Nakhon Pathom (NP). The third measurement set was taken in south Bangkok (BK), on the roof of the Meteorology Building using a CIMEL portable sunphotometer (model CE317) which measured in six spectral bands (Table 1). Data was recorded three times daily (09:00, 12:00, 15:00) for cloudless conditions, encompassing a 2-year period from January 2004 to December 2005. All locations offered an unimpeded sky view greater than 85°. Table 2 summarises the daily data collected.

The Yankee MFRSR allows continuous measurement of direct irradiance as the shadowband provides partitioning of global irradiance into its direct and diffuse component. By contrast, the EKO sunphotometer is outfitted with a sun tracker, therefore providing continuous measurements of direct spectral irradiance. The CIMEL sunphotometer also allows direct measurement of spectral irradiance but this unit was not attached to a sun tracker and, therefore, needed manual measurements on a daily basis, weather permitting. This different observation methodology might affect some of the analysis as discussed in the next section.

Aerosol optical depth and turbidity determinations need cloudless conditions. In Nakhon Pathom, these conditions were determined using a digital sky camera which recorded 180° sky views every half-hour. These data are stored digitally in computer and can be easily retrieved from historical archives. In Bangkok, the Meteorology Department keeps records of total cloud cover and only proceeds with a sunphotometer observation if the sky is cloudless. No cloud records were available at AIT, and in this case cloudless conditions were determined by examining broadband direct beam irradiance and searching for minimum threshold intensities and smoothness in the daily intensity curve.

Each record of sunphotometer data for the three stations is used to derive optical depths and Angstrom coefficients as discussed in the next section. These data are then averaged on a daily basis and used to examine seasonal trends. Table 2 shows the number of days in each month with sunphotometer records. Note that there were a limited number of measurements during the rainy season from June to August.

All three instruments were factory calibrated before the beginning of the field exercise. Nevertheless the extreme precipitation, temperature and humidity of the climate of Bangkok can be harsh on outdoor scientific instruments and there is a possibility that some of the sensors may have deteriorated over the 2-year measurement period. This

Table 2 Number of days in each month with sunphotometer records for each of the three stations

Date	Nakhon Pathom (NP)	Phatum Thani (AIT)	Bangkok (BK)	Date	Nakhon Pathom (NP)	Phatum Thani (AIT)	Bangkok (BK)
Jan 04	9	26	13	Jan 05	23	2	9
Feb 04	4	22	11	Feb 05	27	21	5
Mar 04	10	14	12	Mar 05	23	18	0
Apr 04	15	16	9	Apr 05	24	0	7
May 04	3	16	1	May 05	19	12	1
Jun 04	6	0	3	Jun 05	14	16	3
Jul 04	0	0	2	Jul 05	5	15	2
Aug 04	6	0	1	Aug 05	18	20	2
Sep 04	13	6	0	Sep 05	13	15	0
Oct 04	16	16	16	Oct 05	11	19	8
Nov 04	26	0	7	Nov 05	20	22	9
Dec 04	9	30	20	Dec 05	19	16	2

problem will be examined in the next section which discusses the methodology for obtaining aerosol optical depth.

3 Data analysis

3.1 Aerosol optical depth (AOD)

The well-known Bouguer's law which allows the estimation of the AOD for clear skies is expressed as:

$$I_\lambda = I_{o\lambda} e^{-\tau'_\lambda m_r} \tag{1}$$

where $I_{o\lambda}$ is the extraterrestrial solar irradiance corrected for sun-earth distance, m_r is the relative air mass and τ'_λ are the total atmospheric optical depth. The total atmospheric optical depth can be expressed as

$$\tau'_\lambda = \tau'_{a\lambda} + \tau'_{r\lambda} + \tau'_{o\lambda} + \tau'_{w\lambda} + \tau'_{g\lambda} \tag{2}$$

where $\tau'_{r\lambda}$ is the Rayleigh optical depth, $\tau'_{o\lambda}$ is the optical depth due to the ozone absorption, $\tau'_{w\lambda}$ is the water vapour optical depth, $\tau'_{g\lambda}$ the absorption optical depth due to atmospheric gases (mainly carbon dioxide, nitrogen oxide and carbon monoxide) and $\tau'_{a\lambda}$ is the optical depth due to the extinction by aerosols. We can estimate $\tau'_{a\lambda}$, once we know the values of $\tau'_{r\lambda}$ and $\tau'_{o\lambda}$. The wavelength range 380–870 nm does not include gas or water vapour absorption, so that $\tau'_{w\lambda}$ and $\tau'_{g\lambda}$ may be neglected at these wavelengths. The ozone correction using total column ozone from TOMS/EP is incorporated on the basis of the daily data available on the web.

Neglecting the above two terms, the aerosol optical depth $\tau'_{a\lambda}$ may be written as:

$$\tau'_{a\lambda} = \frac{\left[-\ln \frac{I_\lambda}{I_{0\lambda}} - \tau_{r\lambda} - \tau_{o\lambda}\right]}{m_r} \tag{3}$$

This solution for $\tau'_{a\lambda}$ is essential in contaminated urban environments where aerosol concentrations are not expected to be constant in time, so that a Langley method is not feasible. The negative side is that an exact calibration constant for I_λ is needed as $I_{o\lambda}$ is not determined from the observation, but is deduced from astronomical tables. In the Bangkok environment, the assumption of a stable calibration must be investigated.

A second approach is to assume constant aerosol concentrations at a daily scale and to solve Eq. (1) for $\tau'_{a\lambda}$ using the Langley method (Valiente 1996).

$$\mathrm{In}\left(I'_\lambda\right) = \mathrm{In}\left(I'_{0\lambda}\right) - m\left(\tau'_{r\lambda} + \tau'_{o\lambda} + \tau'_{a\lambda}\right) \tag{4}$$

A plot of $\mathrm{In}\left(I'_\lambda\right)$ vs. m will give the sum of the three optical depths as the slope, from which $\tau'_{a\lambda}$ may be determined. Note that the technique does not rely on an absolute calibration, as the slope is independent of it. It does, however, rely on a stable and constant output for a given spectral radiation energy, a more achievable goal.

3.2 Stability of calibration coefficients during the study period

The procedure followed was to select cloudless days in which aerosol optical depths were obeying the Langley relation as given in Eq. (4). A plot of $\mathrm{In}\left(I'_\lambda\right)$ vs. m should follow a linear relationship over a period of at least 3 h in the morning or afternoon for the regression to be statistically significant. If there has been no calibration drift, the intercept, $\mathrm{In}\left(I'_{0\lambda}\right)$ should be constant for all readings over the 2 years of field measurements and for all the spectral bands of the three instruments. Any deviation from an initial value established on 1 January 2004 is considered a calibration drift. Figure 2 presents the results.

The AIT sunphotometer at 778 nm is the only sensor that exhibits a statistically significant change at the 95% level of confidence. Overall the changes are quite small, with the largest one being the NP sensor at 413 nm (−3.7% change in 2 years), while typically they range between 1 to 2% change over 2 years. These errors would translate as small errors in the determination of $\tau'_{a\lambda}$ if no other error sources are assumed in Eq. (3). They would typically be ±0.02 for an optical depth of 1.0. Figure 2 shows the plot for the 500 nm wavelength at the three stations. Note the lack of trend and the low scatter of the intercept $I'_{0\lambda}$ around the regression line.

Given the above results, it was decided to use the method described in Eq. (3) to obtain aerosol optical depth with no further correction due to sensor deterioration over the 2-year study period.

3.3 Angstrom turbidity coefficient and the wavelength exponent

The aerosol optical depth is related to the Angstrom's turbidity coefficient (β) and the wavelength exponent (α) through the following formula proposed by Angstrom (Iqbal 1983):

$$\tau'_{a\lambda} = \beta\lambda^{-\alpha} \tag{5}$$

Applying Eq. (3) to the computation of aerosol optical depth at λ_1 and λ_2, one can obtain equations relating β and α to the aerosol optical depth as follows:

$$\alpha = \frac{\ln\left(\frac{\tau'_{a\lambda_1}}{\tau'_{a\lambda_2}}\right)}{\ln\left(\frac{\lambda_2}{\lambda_1}\right)} \tag{6}$$

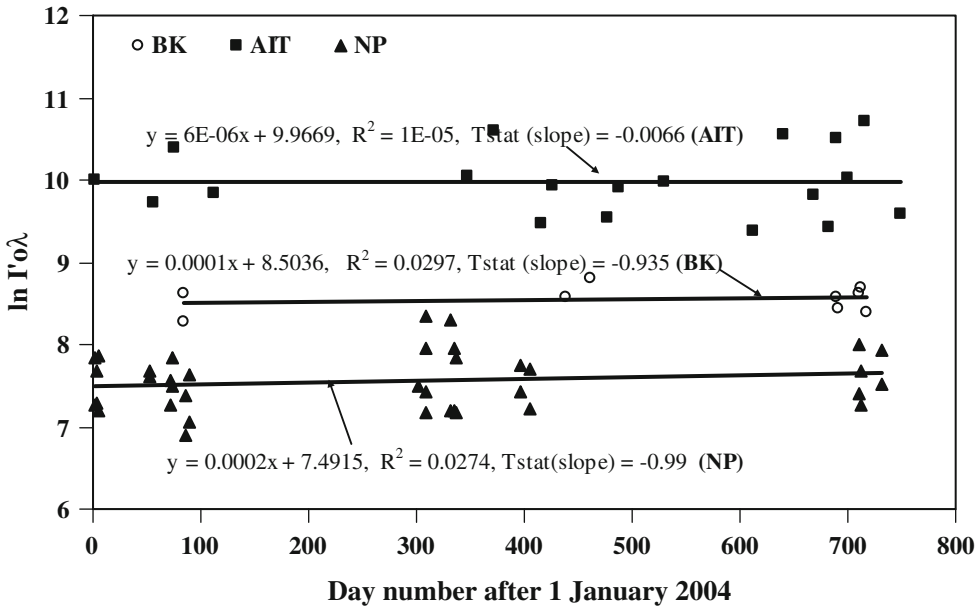

Fig. 2 Regression line for the intercept $I'_{0\lambda}$ obtained in the Langley relationship for 500 nm. None of the changes are significant

and

$$\beta = \frac{\tau'_{a\lambda_1}}{\lambda_1^{-\alpha}} \quad \text{or} \quad \beta = \frac{\tau'_{a\lambda_2}}{\lambda_2^{-\alpha}} \tag{7}$$

where $\tau'_{a\lambda_1}$ and $\tau'_{a\lambda_2}$ are the aerosol optical depth at λ_1 and λ_2, respectively.

There are several choices of wavelength pairs to use in Eqs. (6) and (7) given the multiple channels employed by each instrument. It is also reasonable to choose two wavelengths that are as far apart as possible so as to minimize errors. There is also the need to avoid absorption bands by ozone, noticeable at 500–700 nm (Iqbal 1983). These considerations led to choice of bands 413, 863 nm for Nakhon Pathom, 368 and 778 nm for AIT, and 380 and 870 nm for Bangkok. Using these channels, the Angstrom coefficients α and β were obtained for every day that contained aerosol optical depth data.

4 Results

4.1 Aerosol optical depth

Figure 3a–c presents the AOD results for NP, AIT and BK respectively. A large seasonal trend is evident for the 413 nm wavelength AOD at NP (Fig. 3a), with low AOD in June, July and August, corresponding to the height of the wet season, and very high values approaching 2.0 in March, towards the end of the dry season. There appears to also be some interannual variability, with higher values occurring in March 2005 as opposed to March 2004. For each month of the year, there is considerable variability in AOD, which increases as mean optical depth increases. In March 2005, the range of AOD extends from less than 0.5 to just over 2.0. The seasonal pattern observed in Fig. 3a remains unchanged when higher wavelength bands are considered, but the maximum amplitude of the AOD changes keep getting smaller as the wavelength increases. At 863 nm, all AOD are at 0.5 or less.

The 368 nm AOD pattern for the AIT instrument at Phatum Thani (Fig. 3b) exhibits some similarity to the 413-nm pattern at Nakhon Pathom (NP). There is a peak in AOD in January and February 2005 in the dry season, but lower values in June, July and August 2005, during the wet season. There are also gaps with no data available in June, July and August 2004 and April 2005, indicating the absence of cloudless days. This feature is likely to result from the cloud detection protocol that had to be used at AIT in the absence of direct cloud observations. As in Nakhon Pathom, AOD decreases with increasing wavelength band, reaching values of 0.5 or lower at a wavelength band of 778 nm.

The variability of AOD for Bangkok (BK) is different from the other two sites (Fig. 3c). The seasonal pattern is not as distinct, but this might be a result of the very few manual measurements that were taken during the wet season. Furthermore, during the dry season, the variability in the short wavelength band (380 nm) is larger than at the two sites, which is a result of much lower measured values at the bottom end of the measurement scale. In other words, the site recorded AOD values that ranged from mildly turbid to very turbid. At larger wavelengths bands the AOD values decrease on average, but for any given month, the lower measured values at the bottom end still persist.

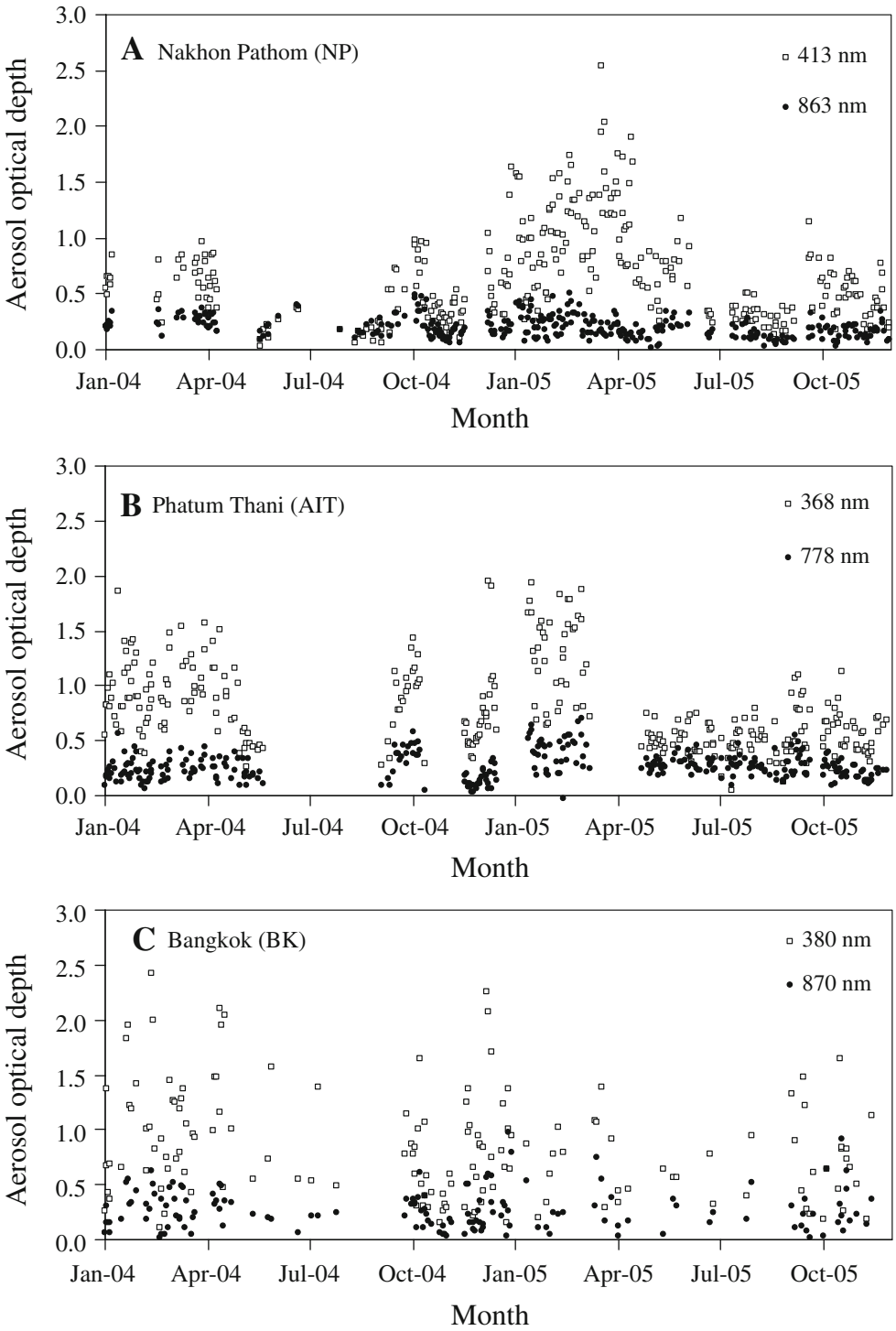

Fig. 3 Daily variation of aerosol optical depth for: **a** Nakhon Pathom, *NP* **b** Phatum Thani, *AIT* and **c** Bangkok, *BK*. For ease of viewing, only the optical depth of the lowest and the highest wavelength are shown

4.2 Angstrom turbidity coefficients

As mentioned previously, Eqs. (6) and (7) were solved with every determination of AOD so as to get the Angstrom wavelength exponent α and the turbidity coefficient β. Examining the variability of α first (Fig. 4), it may be observed that it also goes through a seasonal cycle, reaching maximum values of between 2 and 3 in all stations at the height of the dry season. At the other extreme end, quite low values are obtained during the wet season,

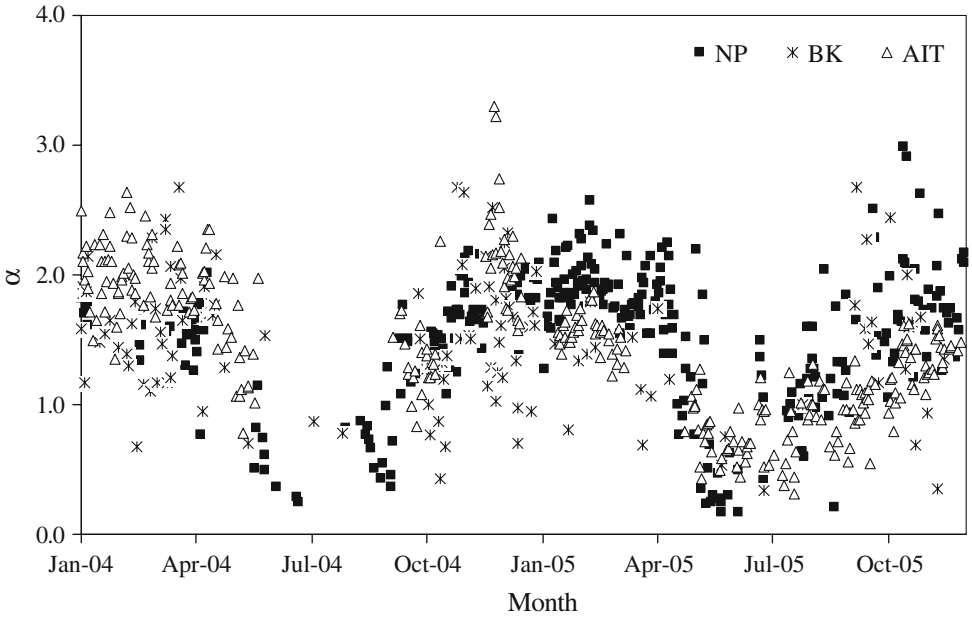

Fig. 4 Daily variability of the wavelength exponent (α) for Nakhon Pathom, Phatum Thani and Bangkok

with all three stations recording values of 0.5 or less. One noticeable feature is the greater scatter occurring in the Bangkok (BK) station for all seasons.

The pattern of variability is much less clear for the turbidity coefficient β (Fig. 5). No obvious pattern appears at NP or BK, while at AIT there is a pattern of decreasing β after February 2005.

4.3 Daily variability

It is also of interest to examine how AOD changes at a daily time scale. It is expected that there will be many complex processes operating, so that it is unlikely that a single pattern will emerge. Examining sources, there are the usual anthropogenic sources related to urban areas such as motor-vehicle emissions, industrial emissions, domestic activities (burning of backyard rubbish, paint spraying, etc.) and others. There should be no distinct seasonal variability in emissions, and although it is expected that vehicle emissions should be lower on weekends, no cyclic variations appeared at the weekly time scale. A second and important source is photochemical reactions from industries or biomass burning, resulting in complex interactions between hydrocarbons, ultraviolet radiation and nitrogen

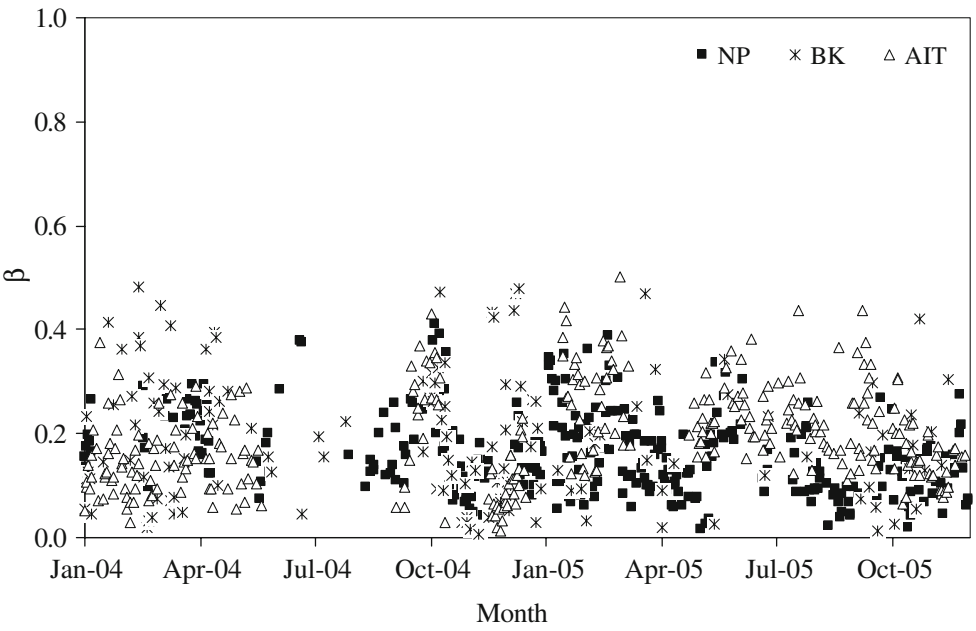

Fig. 5 Daily variability of the Angstrom turbidity coefficient parameter (β) for Nakhon Pathom, Phatum Thani and Bangkok

oxides in the boundary layer (Oke 1987). Photochemical reactions increase with solar radiation, but there are delay times, so that it may extend beyond the solar radiation cycle. Sinks relate to gravity deposition on the surface, impaction on the surface, adhesion of two or more suspended aerosols to form a larger one, and advective transport by wind to other areas. Essentially concentrations (and AOD) will be a result of the interplay between sources and sinks.

To observe diurnal changes, continuous data records for NP and AIT were examined. Records for BK were not used as it was considered that three daily observations were insufficient for the analysis. Days which have "complete" daily records were used, with "complete" denoting days with observations in the three time periods 7:00–9:00, 11:00–13:00, and 15:00–17:00. AOD in each time period was averaged regardless of the length of record in each period. Differences were then calculated between the average AOD at noon (11:00–13:00) minus the morning AOD (7:00–9:00); and between the AOD in the afternoon (15:00–17:00) and noon (11:00–13:00). This procedure was used in the lowest wavelength bands (413 nm and 368 nm) and a high wavelength band (671, 675 nm). Finally, only the period November to April was used, the reason being that precipitation in the wet season would be quite erratic, making diurnal changes difficult to observe.

Results are presented in Fig. 6a–d. They are shown as frequency distribution of the AOD difference (ΔAOD) between noontime and morning or afternoon and noon AODs. It is evident that the AOD is far from constant. Examining the NP instrument at 413 nm, it may be noticed that both morning and afternoon changes show the predominance of increases in AOD as opposed to decreases. All the afternoon changes are positive, while the morning registers 79% positive changes. We interpret this result as indicating the dominance of source terms—photochemical reactions persisting all day. The case for NP at longer wavelength is more complex. Keeping in mind that the smog-producing processes are less important in these wavelengths, it is seen that morning changes *decrease*, while afternoon changes *increase* on average. It is possible that in the morning scenario, the sink terms via increased wind speed and boundary layer growth is larger than the weaker rate of photochemical production. Afternoon changes, however, show increases, indicating the importance of the photochemical and other source terms.

The AIT pattern shows more variability. The morning period exhibits more decreases compared to NP. Sink terms such as wind effects may be stronger here. Forty seven percent of occasions report increases at 368 nm. By contrast, 62% of occasions at 675 nm exhibit increases.

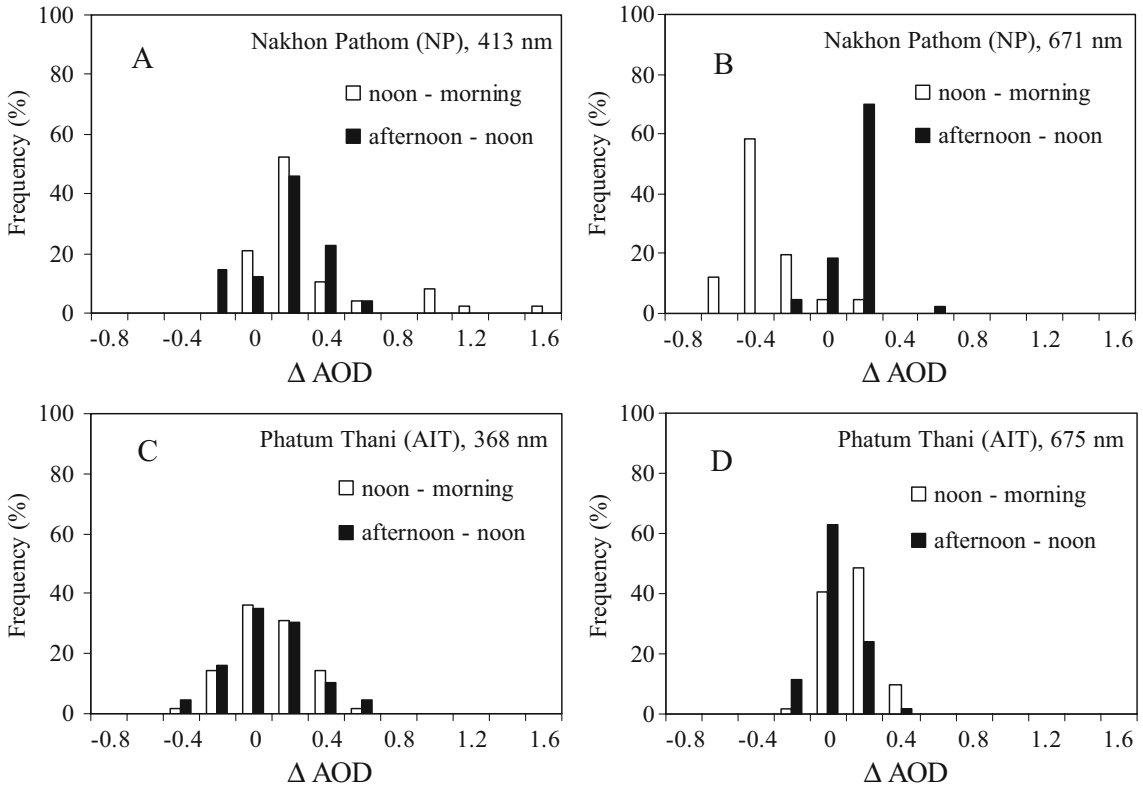

Fig. 6 Frequency of changes of aerosol optical depth (ΔAOD) for **a** Nakhon Pathom at 413 nm, **b** Nakhon Pathom at 671 nm, **c** AIT at 368 nm, and **d** AIT at 675 nm. Differences have been calculated by obtaining averages for the time intervals 7:00–9:00 (morning), 11:00–13:00 (noon), and 15:00–17:00 (afternoon)

Table 3 Experimental details for the 2 days that were modeled at Nakhon Pathom

Date	Optical depth for different wavelengths					Precipitable water (cm)	Ozone (DU)
	413 nm	500 nm	613 nm	671 nm	864 nm		
9 Mar 05	1.482	1.188	0.923	0.834	0.488	2.8	274
19 Nov 04	0.309	0.351	0.252	0.184	0.146	4.0	258

Optical depths were daily averages. See text for details of data on precipitable water vapour and total column ozone (Ozone).

The afternoon period is evenly distributed at 675 nm, but decreases dominate in the afternoon at 368 nm.

To summarize, no clear pattern emerges as the two stations show different results. Aerosol optical depth shows both increases and decreases in the mornings and afternoons. Changes also appear to be dependent on aerosol optical depth, but the results are equivocal when the two stations are considered. Clearly a more detailed analysis using local meteorological data is needed. However this task is beyond the scope of the present study.

4.4 Depletion of global radiation

In this section, we examine what the typical aerosol effects on the global and direct broadband radiation are in the region. It is an important quantity as a heavy aerosol load may affect the amount of photosynthetically active radiation (PAR) available at the surface, or the total solar energy available for partitioning by the surface into sensible, latent or soil heat flux (Oke 1987). Two days were examined in Nakhon Pathom which spanned a range of aerosol loads as given by the measured optical depths. Aerosol optical depth measured for each day was used in a radiative transfer model which produced direct and diffuse broadband solar radiation. Additionally, the model was applied with the same meteorological conditions except for the clean, aerosol-free conditions. We treat the ratio of the polluted to clean irradiance as a measure of depletion by the aerosol layer.

Table 3 provides details of the input parameters for the two selected days. Aerosol optical depth for 9 March 2005 was relatively high and typical of the late dry season. Data for 19 November 2004 was much lower, as is expected at the end of the wet season. Precipitable water-vapour data for Nakhon Pathom was obtained from the NOAA Climate Data Centre (http://www.cdc.noaa.gov), and daily column ozone from the TOMS web site at http://toms.gsfc.nasa.gov.

The radiative transfer model also required spectral albedos for our experimental site. They were obtained from the NASA web site of the Surface and Atmosphere Radiation Budget (SARB) group (http://www-surf.larc.nasa.gov) which produced 20 surface albedos for the Earth following the International Global Biosphere (IGBP) scene types. According to the Department of Agricultural Extension (http://www.doae.go.th/stat/bsck/frmsc.htm), Nakhon Pathom province representing an area of 1,565 km^2 (see Fig. 1), has approximately 55% of its surface urbanized. In the model input, we used a spectral albedo made up of a combination of the IGBP "urban type" (55%) and "cropland" (45%).

The "streamer" radiative transfer model was used in the analysis (Key and Schweiger 1998). It uses a discrete ordinate solver (DISORT), and offers a choice of multiple streams (we used eight), 24 shortwave bands, gaseous absorption, spectral albedos and a variety of model atmospheres with aerosol components. The user may input aerosol optical depth at 600 nm, precipitable water and total column ozone. In this study, we have used a tropical atmosphere with smoke aerosols and high troposphere load.

Table 4 presents the results. Daily irradiance on the high-aerosol day, 9 March, is only 63% of that expected in a totally aerosol-free day. Much of the direct radiation is depleted, so that only 44% of the direct irradiance expected for the clear day is transmitted. Most of the direct radiation

Table 4 Output from the Streamer model for two aerosol days. *I*, *D* and *G* stand for direct, diffuse and global irradiance, respectively

Date	Model						Daily measurements		
	Daily			Noon					
	I_a/I_0	D_a/D_0	G_a/G_0	I_a/I_0	D_a/D_0	G_a/G_0	G_a/G_m	I_a/G_a	I_m/G_m
9 Mar 05	0.44	2.99	0.63	0.50	3.76	0.69	0.96	0.65	0.49
19 Nov 04	0.72	2.48	0.87	0.77	2.82	0.90	1.03	0.92	0.78

Subscripts a, 0 and m stand for model aerosol, model without aerosol and measured, respectively. Data are presented as daily averages, at solar noon and as daily averages compared with measurements

is transmitted in a forward direction, therefore increasing the diffuse irradiance. Higher transmissions are seen at solar noon which is very likely a result of the lower air mass. Transmissions are also higher on the cleaner day, 19 November, with 87 and 72% for the daily global and direct transmissions, respectively.

Table 4 also shows how model output compares with measurements. In terms of global radiation, model and measurement match with an error equal to or less than 4%. However larger errors appear in partitioning the global radiation, as the model tends to overestimate the fraction of global radiation that is direct. Clearly, more detailed knowledge of the aerosol optical properties are needed to lower the error in the partitioning of global radiation.

5 Discussion

It is evident that AOD has undergone seasonal changes at NP and AIT measurement stations. Precipitation during the wet season scavenges many aerosols from the atmosphere, lowering the AOD at all wavelength bands. As the year progresses into the dry season, there is less scavenging from precipitation and the AODs increase, reaching a maximum sometime in late March and early April. The optical depth for any one day during any season decreases with wavelength, which indicates the predominance of small particles in direct beam depletion.

Monthly average optical depths for 500 nm are plotted for AIT, NP and BK as a time series graph. The agreement between the three series shown in Fig. 7 is encouraging, considering that different instruments are involved at different sites in a heavily contaminated environment. All three measurement sequences follow the seasonal trends and there is also broad agreement in the absolute values. One large difference occurs in January 2005 when an AOD of 1.12 is measured at AIT as compared to 0.66 measured at NP and 0.60 and BK. In fact, the large average value at AIT is based on two measurements taken on 30–31 January 2005. By contrast the NP and BK averages are based on 23 days and 9 measurement days respectively (Table 2). So it is likely that even better agreement may be obtained with a longer cloudless data set, perhaps based on several years of measurement.

One notable feature in the BK AOD series is the higher range of AOD measured especially in the dry season resulting in lower AOD at the bottom end of the scale. Examining the geographic location of the site, it may be observed that it is quite close to the sea, approximately 20 km (Fig. 1). During November and December, approximately half of the days report wind directions from the south, and it is possible that the maritime air mass is transporting lower aerosol concentrations. The hypothesis was tested by grouping the 500-nm AOD data into northerly and southerly sectors and observing the difference in the frequency distribution of 500 nm AOD. However, results showed no statistical difference between the two data sets. Nevertheless it is possible that a more complex wind flow may be occurring which may go some way towards explaining the results.

The AOD data presented here are high, but similar results have been reported by Zhang and Mao (1999) from a station close to Beijing using sun photometers. The 1-year study showed that maximum AOD was reached during the dry season, reaching maximum values of just over 1.0 at 550 nm. The results are in good agreement with our measurements at NP and AIT, but the BK data exhibit even larger AOD at 500 nm.

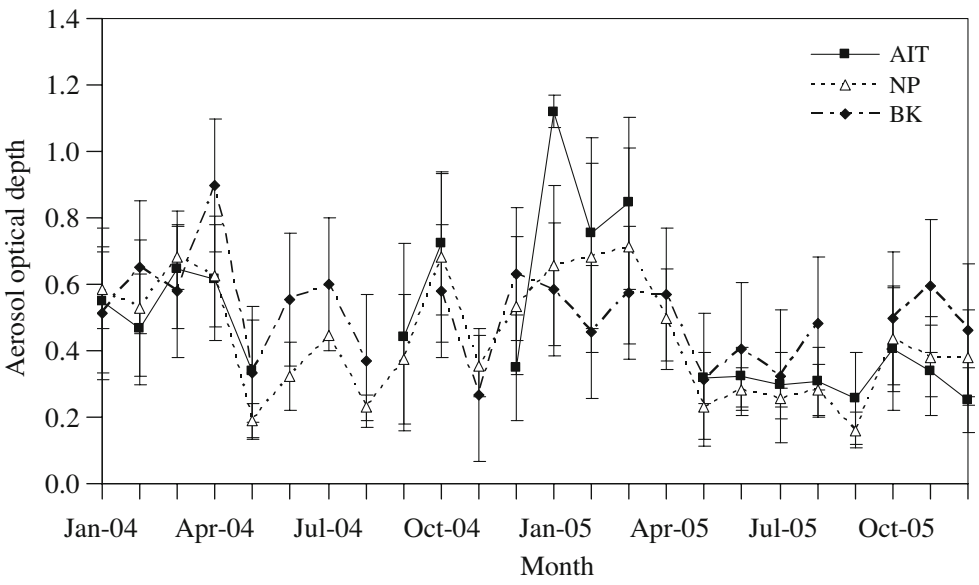

Fig. 7 Monthly average aerosol optical depth at 500 nm for Nakhon Pathom (*NP*), Phatum Thani (*AIT*) and Bangkok (*BK*) sites. Also shown are the monthly standard deviations. Aerosol optical depth data for July 2004 represents only one observation and has no standard deviation

It is interesting to note that the Angstrom exponent α also shows seasonal changes. To examine this process further, AOD is plotted vs. α in the lowest wavelength band at all three stations (Fig. 8). The data were partitioned into a dry season from December to February and a wet season from May to September. As may be observed, the relationships are very different for the two seasons. During the wet season there are increases in α with AOD. It is clearly seen in the AIT and BK pattern, while the NP shows increases, although there is considerably more scatter. By contrast all three stations exhibit constant or slight increases in α with decreasing AOD during the dry season, but reaching a quasi-constant value at AODs between 1.5 to 2.

It is likely that the two different patterns are related to moisture conditions in the atmosphere. Alpha increases with optical depth during the wet season, typified by air masses that originate in the Indian Ocean. The size distribution is very homogeneous and α is low following

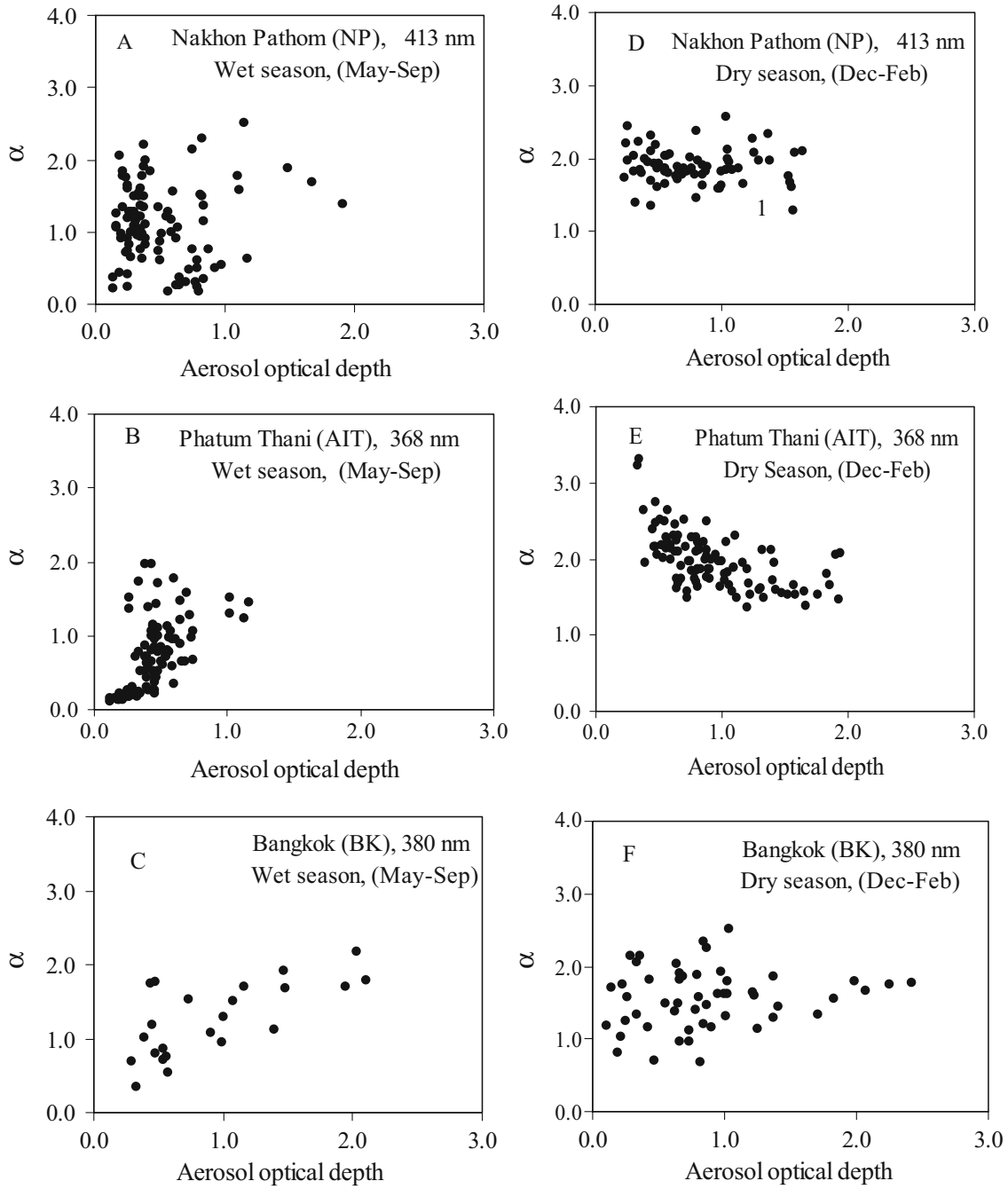

Fig. 8 Relationship between daily aerosol optical depth and wavelength exponent (α) for the wet season in Nakhon Pathom (**a**), Phatum Thani (**b**), Bangkok (**c**), and aerosol optical depth and α for the dry season in Nakhon Pathom (**d**), Phatum Thani (**e**) and Bangkok (**f**)

aerosol scavenging by rain events. Photochemical production is very active in the days following the rain event and as a result, smaller size particles increasingly dominate the size spectrum and AOD's become larger. The pattern in the dry season is very different as aerosol optical depths remain high, fine particles dominate with high α values, and the aerosols are continental in origin (Zhang and Mao 1999). In addition, it is expected that photochemical processes are also active, emphasizing the smaller particle range.

The seasonal pattern for β (Fig. 5) is much less clear than that for α in Fig. 4. While all three stations report decreasing α values in the wet season from May to September, this is not strictly the case for β. In particular, high values are reported in October 2004 and low values again in November 2004. By contrast, α values continue to increase during this time period. Other peaks in β are reported in June 2005, at the height of the wet season. These results indicate that the sources (and processes) governing the total number of particles are much more varied than those governing the size distribution α.

Diurnal changes in AOD (Fig. 6) also reveal some interesting changes in the Angstrom coefficients. As most of the data of Fig. 6 was obtained during the dry season, we can infer changes in α and β using Fig. 8, which plots α vs. AOD. Positive increases in AOD at NP for noon-morning and afternoon-noon (Fig. 6a) indicate that β is likely to increase since α is largely constant with AOD (Fig. 8d). This equates to production of a higher number of particles as the day progresses. At AIT the process is similar with high AOD, greater than 1. However Fig. 6c indicates that there is no dominant trend in either morning or afternoon changes.

Studies which examine AOD characteristics are scarce for tropical or sub-tropical regions. Some relevant statistics are reported by Maduekwe and Chendo (1997) in Lagos, Nigeria. Lagos is a tropical city with a dry and wet season, shaped by two distinct air masses originating in the Sahara and in the tropical Atlantic respectively. They report a lowest monthly average "clearness index" of 0.45 for January, during the dry season. This index is defined as the ratio of the extra-terrestrial daily solar radiation to that received at the surface in cloudless conditions. Using this definition, our clearness index for 9 March in Table 4 converts to 0.51, approximately 13% higher than their value. Their indices for the wet season range from 0.45 to 0.65, with averages close to 0.6. This average figure is slightly lower than our low value of 0.66 for 19 November at the end of the wet season.

Statistics on the Angstrom coefficients have also been reported by Maduekwe and Chendo (1997). Monthly values of β range from 0.5 for January to 0.3 for June. Zakey et al. (2004) obtain monthly values for β in Cairo, Egypt, which vary by 0.20–0.25, with the highest values being influenced by spring desert storms. Tadros et al. (2002), also working in Cairo, give a yearly average figure of 0.283 for β. Highest monthly values presented in this study for the three stations range from 0.21 to 0.26, and they appear to be similar in magnitude to the Cairo studies. However, our yearly average figures are lower (0.16–0.20), indicating monthly variability during the year. Grouping data from all three stations together, monthly average α, ranges from 0.6 to 2.0. These values are contained inside the range of 0.91–3.2 reported for Lagos, Nigeria by Maduekwe and Chendo (1997).

6 Conclusion

This study has examined the spatial and temporal variability of aerosol optical properties in the Bangkok Metropolitan area. Analysis of the sun photometers showed a marked change in aerosol optical depth for all bands. They are lowest in October/November and gradually increase during the dry season, reaching maximum values in late March and early April. The Angstrom exponent α also undergoes a seasonal variation, with maximum values in the dry season and minimum values at the height of the wet season. There is much more scatter in the seasonal pattern of the turbidity coefficient β, with maximum and minimum peaks occurring at various times of the year.

The sources for the pollution are largely unknown and remain a challenge, as they have not been specifically examined for the Thailand environment. However studies done in neighboring Malaysia (von Hoyningen-Huene et al. 1999) and in the Amazon basin (Holben et al. 1996) indicate that biomass burning increases significantly the optical depth, produces aerosols of low single scattering albedo, and has a negative forcing effect on the surface shortwave radiation. In Thailand much of the biomass burning occurs in January-April as rice straws are burnt after harvesting.

Work is underway to obtain more information on the optical properties of these aerosols. A new network of Cimel sunphotometers has recently been established for Thailand. These instruments provide detailed information not only of aerosol optical depth, but can also estimate other important properties such as the single scattering albedo, the complex index of refraction, the phase function and the size distribution. These data will help us understand the nature of these aerosols, their sources and their likely impact on the climate of our region.

Acknowledgements The authors would like to thank the Thailand Research Fund (TRF) for the financial support to carry out this research work. The authors also would like to thank Prof. S. Chirarattananon, Dr. P. Chaiwiwatworakul and Ms. S. Sudhibrabha for providing spectral data at AIT and Bangkok.

References

Angstrom A (1929) On the atmospheric transmission of sun radiation and dust in the air. Geograph Annal 2:156–166

Angstrom A (1964) The parameters of atmospheric turbidity. Tellus 16:64–75

Holben BN, Setzer A, Eck TF, Pereira A, Slutsker L (1996) Effects of dry season biomass burning on Amazon basin aerosol concentrations and optical properties. J Geophys Res 110(D144):19465–19481

Iqbal M (1983) An introduction to solar radiation. Academic, New York

Kaufman YJ, Gitelson A, Karnieli A, Ganor E, Fraser RS, Nakajima T, Mattoo S, Holben BN (1994) Size distribution and phase function of aerosol particles retrieved from sky brightness measurements. J Geophys Res 99(10):10341–10356

Key J, Schweiger AJ (1998) Tools for atmospheric radiative transfer: streamer and fluxnet. Comput Geosci 24(5):443–451

Maduekwe AAL, Chendo MAC (1997) Atmospheric turbidity and diffuse irradiance in Lagos, Nigeria. Sol Energy 61:241–249

Masmoudi M, Chaabane M, Medhioub K, Elleuch F (2003) Variability of aerosol optical thickness and atmospheric turbidity in Tunisia. Atmos Res 66:175–188

NEPC (National Environment Protection Council) (1997) Draft National Environment Protection measure and impact for air quality, National Environmental Protection Council Report, NEPC, Adelaide, Australia

Oke TR (1987) Boundary layer climates. Methuen, New York

Ramachandran S, Jayaraman A (2003) Spectral aerosol optical depths over bay of Bengal and Chennai: I- measurements. Atmos Environ 37:1941–1949

Tadros MTY, El-Metwally M, Hamed AB (2002) Determination of Angstrom coefficients from spectral aerosol optical depth at two sites in Egypt. Renew Energy 27:621–645

Valiente JA (1996) A study and parameterization of oceanic aerosol interaction by interpreting spectral solar radiation measurement at Nauru during TOGA-COARE. PhD Thesis, Tasmania University, Australia

Von Hoyningen-Huene W, Schmidt T, Schienbein S, Kee CA, Tick LJ (1999) Climate-relevant aerosol parameters of South-East Asian forest fire haze. Atmos Env 33:3183–3190

Xin J, Wang S, Wang Y, Yuan J, Zhang W, Sun Y (2005) Optical properties and size distribution of aerosols over the Tengger Desert in northern China. Atmos Environ 39:5971–5978

Zakey AS, Abdelwahab MM, Makar PA (2004) Atmospheric turbidity over Egypt. Atmos Environ 38:1579–1591

Zhang J, Mao J (1999) Remote sensing aerosol optical depth from space and ground. Proc. of the 20th Asian Conference on Remote Sensing, 22–25 November 1999, Hong Kong, China, pp 1–7